

## Heteroepitaxial Growth of Single 3C-SiC Thin Films on Si (100) Substrates Using a Single-Source Precursor of Hexamethyldisilane by APCVD

Gwiy-Sang Chung\* and Kang-San Kim

School of Electrical Engineering, University of Ulsan, Ulsan 680-749, Korea. \*E-mail: gschung@ulsan.ac.kr  
Received March 30, 2006

This paper describes the heteroepitaxial growth of single-crystalline 3C-SiC (cubic silicon carbide) thin films on Si (100) wafers by atmospheric pressure chemical vapor deposition (APCVD) at 1350 °C for micro/nanoelectromechanical system (M/NEMS) applications, in which hexamethyldisilane (HMDS, Si<sub>2</sub>(CH<sub>3</sub>)<sub>6</sub>) was used as a safe organosilane single-source precursor. The HMDS flow rate was 0.5 sccm and the H<sub>2</sub> carrier gas flow rate was 2.5 slm. The HMDS flow rate was important in obtaining a mirror-like crystalline surface. The growth rate of the 3C-SiC film in this work was 4.3 μm/h. A 3C-SiC epitaxial film grown on the Si (100) substrate was characterized by X-ray diffraction (XRD), transmission electron microscopy (TEM), reflection high energy electron diffraction (RHEED), atomic force microscopy (AFM), X-ray photoelectron spectroscopy (XPS) and Raman scattering, respectively. These results show that the main chemical components of the grown film were single-crystalline 3C-SiC layers. The 3C-SiC film had a very good crystal quality without twins, defects or dislocations, and a very low residual stress.

**Key Words :** Heteroepitaxial growth, Cubic silicon carbide (3C-SiC), Hexamethyldisilane (HMDS, Si<sub>2</sub>(CH<sub>3</sub>)<sub>6</sub>), Chemical vapor deposition (CVD)

### Introduction

In recent years, many electronic and mechanical micro-devices that can be used at high temperatures and in corrosive environments are being particularly demanded by fields involved in automotive, aerospace, ships, nuclear power instrumentation, satellites, space exploration, and geothermal wells.<sup>1</sup> Among various semiconductor materials, silicon carbide (SiC) is an attractive material for high power, high voltage, high frequency and high temperature microelectronics, owing in part to its wide band gap, high thermal conductivity, high break down field and high saturation velocity.<sup>2</sup> Compared with Si or GaAs, it is chemically inert, extremely hard, radiation-resistant, and highly wear-resistant making it is possible to fabricate microsensors and micro-actuators for harsh environments such as high temperature, aggressive and corrosive media, and radiation-exposed environments.<sup>3,4</sup> In particular, cubic SiC is an excellent candidate for microelectromechanical systems (MEMS) operating in extreme surroundings because of its excellent chemical, thermal and mechanical properties at high temperatures.<sup>5,6</sup> Additionally, SiC is inert to most chemicals at room temperature and has been found to be biocompatible with inert to bacterial growth,<sup>7</sup> transparent to visible light, and radiation-hard, and to show UV wavelength absorption.<sup>8</sup> Furthermore, owing to its large ratio of Young's modulus to density, SiC has also attracted interest for use in ultra high-frequency nanoelectromechanical system (NEMS) for wireless signal-processing systems.<sup>9,10</sup>

Chemical vapor deposition (CVD) has been mainly used in growing heteroepitaxially single-crystalline SiC thin films on carbonized Si wafers despite the large lattice mismatch (~20%) and the difference of thermal expansion coefficient

(~8%) between 3C-SiC layer and Si substrate.<sup>11</sup> A high density of defects, such as misfit dislocations, stacking faults and anti-phase boundaries, and a high residual stress exist in the SiC film grown on Si substrates. Despite these disadvantages, a technique of producing large area SiC layers by heteroepitaxial growth on Si substrates has been developed, making high-volume batch processing possible, thus allowing the use of highly advanced Si micromachining in M/NEMS fabrications.<sup>12</sup> The application of a heteroepitaxial 3C-SiC film grown on Si wafers in the M/NEMS fields can be of great interest in fabricating new microsensors and microactuators for harsh environments, RF and bio fields in conjunction with Si micromachining technology.<sup>13</sup>

Up to now, significant process has been made in the growth of single-crystalline SiC bulk films, with special emphasis on the 6H- and 4H-hexagonal polytypes, and 3C-cubic polytype. The most common precursors for 3C-SiC films are double-source precursors such as SiH<sub>4</sub> (or SiHCl<sub>3</sub>) and C<sub>3</sub>H<sub>8</sub> (or CH<sub>4</sub>) with a carrier gas (H<sub>2</sub>), usually at temperatures higher than 1200 °C.<sup>14</sup> However, strict safety control is required for the use of silane gas source owing to its explosive nature, flammability and toxicity. To overcome these serious problems, a single organosilane precursor such as tetraethylsilane (TMS, Si(CH<sub>3</sub>)<sub>4</sub>)<sup>15</sup> or hexamethyldisilane (HMDS, Si<sub>2</sub>(CH<sub>3</sub>)<sub>6</sub>)<sup>16</sup> has been used in growing 3C-SiC thin films due to its safety, ease of handling, low growth temperature and accurate stoichiometry recently. Moreover, low pressure (LPCVD) below 10 Torr is superior to an atmospheric pressure (APCVD) because it is possible to grow thin films with uniform and smooth morphology during the 3C-SiC film growth. However, in spite of these advantages, LPCVD has disadvantages of low growth rate and an additional cost of establishing and maintaining low pressure. In

this work, single-crystalline 3C-SiC epilayers were grown on Si (100) wafers up to 17.5  $\mu\text{m}$  using a single-source precursor of HMDS by APCVD for M/NEMS applications.

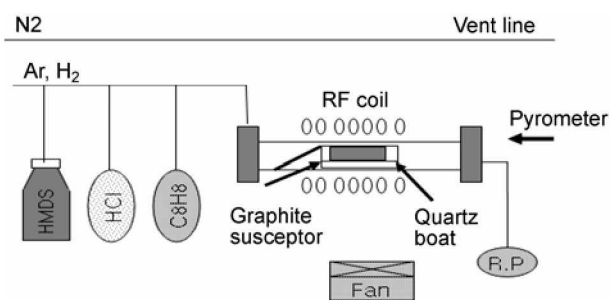
### Experimental Section

Figure 1 shows a schematic diagram of the conventional APCVD used for 3C-SiC growth. Briefly, the reactor consisted of an air-cooled horizontal quartz tube (50 mm inner diameter, 200 mm long) connected to a rotary pump. Si (100) substrates were loaded to a SiC-coated graphite susceptor supported by a quartz boat to event the contamination of the inner reactor and heated by RF induction 4 KW and 40 KHz. The temperature of the substrate was measured through the quartz tube using an optical pyrometer. The reaction tube and graphite susceptor were evacuated to 0.1 Torr, purged with  $\text{H}_2$  carrier gas and preheated at 1350  $^\circ\text{C}$  for 15 min before the growth.

A Si (100) substrate with an on-axis was used for the growth of 3C-SiC thin films. Prior to deposition, the substrate was dipped in concentrated HF to remove native oxide, rinsed with deionized water, and dried in  $\text{N}_2$  flow. A Si wafer was laid horizontally, parallel to the gas flow on the susceptor at the center of the hot-wall zone of the reactor tube, as shown in Figure 1.

A single organosilane precursor using HMDS with a purity of 99.99% (4 N) was used as the source containing directly bonded Si and C atoms during 3C-SiC growth. Ar and  $\text{H}_2$  were used as the purging and carrier gases, respectively. HMDS was transferred to the reactor by bubbling its container with  $\text{H}_2$  at 20  $^\circ\text{C}$  at controlled flow rate and decomposed at a low temperature of about 750  $^\circ\text{C}$ .<sup>16</sup> The vapor pressure of HMDS was about 3.0 kPa in this state.

Figure 2 shows the temperature and gas flow profiles for 3C-SiC growth sequences. All the experiments reported here were performed at atmospheric pressure during growth. Before deposition, the reactor and graphite susceptor were degassed at 1380  $^\circ\text{C}$  for 15 min to minimize outgassing from the surface of the reactor and susceptor. The overall growth consisted of three steps: Firstly, the substrate was heated to 1170  $^\circ\text{C}$ , kept at this temperature for 11 min, and etched in a mixture of HCl and  $\text{H}_2$  to remove the protective oxide layer; the flow rates of HCl and  $\text{H}_2$  were 63.1 sccm and 1 slm, respectively. Secondly, the carbonization of the substrate



**Figure 1.** Schematic diagram of the APCVD used for 3C-SiC growth using single-source precursor of HMDS.

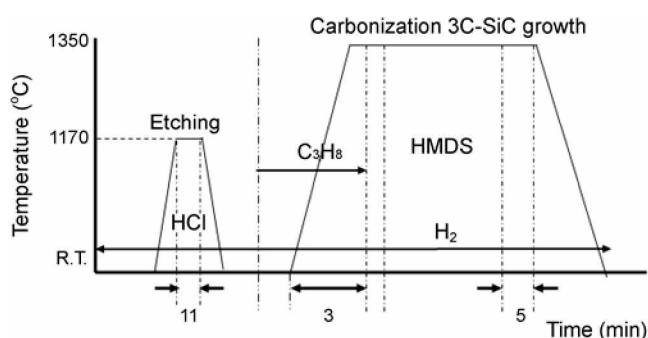


**Figure 2.** A schematic of the temperature and gas flow profiles for 3C-SiC growth process.

prior to 3C-SiC deposition was then performed by introducing  $\text{C}_3\text{H}_8$  into the reactor. The susceptor temperature was increased from room temperature to 1350  $^\circ\text{C}$  for 3 min in a mixture of  $\text{C}_3\text{H}_8$  and  $\text{H}_2$ , in which the flow rates of  $\text{C}_3\text{H}_8$  and  $\text{H}_2$  were 1.0 sccm and 1 slm, respectively. The temperature of 1350  $^\circ\text{C}$  was maintained for 2 min. After carbonization, HMDS gas was immediately introduced for the growth of 3C-SiC films at 1350  $^\circ\text{C}$  for 1 h; the flow rates of HMDS and  $\text{H}_2$  were 0.5 sccm and 2.5 slm, respectively. Finally, the deposition was completed by turning off the HMDS flow, and temperature was kept at 1350  $^\circ\text{C}$  for 5 min in order to stabilize the 3C-SiC films after growth, and followed by the cooling of the substrate to room temperature in a  $\text{H}_2$  flow of 2.5 slm. In this work, the growth rate of 3C-SiC films was about 4.3  $\mu\text{m}/\text{h}$ , which is faster than that of double-source precursors such as  $\text{SiH}_4$  (or  $\text{SiHCl}_3$ ) and  $\text{C}_3\text{H}_8$ .<sup>13,14</sup>

The surface morphology of the grown 3C-SiC films was observed by Nomarski optical microscopy and atomic force microscopy (AFM). The thickness of the films was measured using a spectroscopic ellipsometer and scanning electron microscopy (SEM). The crystallinity of the grown films was determined by X-ray diffraction (XRD), reflection high-energy electron diffraction (RHEED) analyses, transmission electron microscopy (TEM), and X-ray photoelectron spectroscopy (XPS). Raman spectroscopy was also used to investigate the existence of excess carbon in the films.

### Results and Discussion

Figure 3(a) shows typical XRD spectra for 4.3- $\mu\text{m}$ -thick 3C-SiC (100) films grown on the Si (100) substrate at 1350  $^\circ\text{C}$ . A single sharp SiC (002) peak appeared at  $2\theta = 41.4^\circ$  and Si (004) peak at  $2\theta = 69.2^\circ$  corresponded to the Si (100) substrate. This result was consistent with previously reported data.<sup>17</sup> However, no other peaks were detected from the XRD spectra, indicating that single-crystalline cubic SiC (100) films were heteroepitaxially grown on the Si (100) substrate from a single-precursor of HMDS at 1350  $^\circ\text{C}$ . Moreover, an X-ray rocking curve measurement of the grown 3C-SiC films was carried out and the full width at half maximum (FWHM) of the films was examined. The direction of incidence of X-ray was parallel to the  $\langle 110 \rangle$  azimuth of the substrate. Figure 3(b) shows an FWHM of the SiC

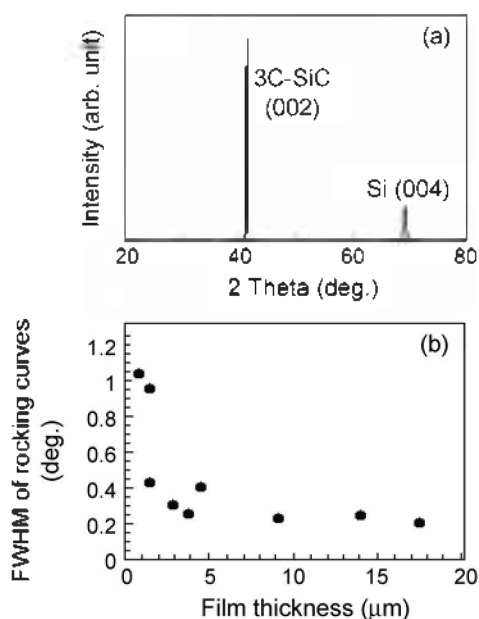


**Figure 3.** Typical (a) X-ray diffraction spectra of 4.3- $\mu\text{m}$ -thick 3C-SiC film grown on Si (100) substrate at 1350 °C and (b) variation in FWHM of SiC (002) X-ray rocking curves depending on 3C-SiC film thickness.

(002) X-ray rocking curves depending on the thickness of grown 3C-SiC films. With increasing SiC film thickness from 0.6 to 17.5  $\mu\text{m}$ , FWHM varied from 1.05 to 0.18 degrees. Particularly, FWHM decreased rapidly as SiC film thickness increased from 0.6 to about 3.0  $\mu\text{m}$ . This indicates that the crystallinity of the grown 3C-SiC epilayers rapidly improved as the SiC film thickness increased up to about 3.0  $\mu\text{m}$ . We consider that the 3C-SiC film grown with a thickness greater than 3.0  $\mu\text{m}$  has the best quality.

Figures 4(a) and (b) show plane and dark-field cross-sectional TEM images of the 3C-SiC films grown on the Si (100) substrate by APCVD. It is evident that the 3C-SiC film grown on the Si (100) substrate has very good single-crystalline quality without grain boundaries, as shown in Figure 4(a). Moreover, many multilayer defects and dislocations in the SiC film are due to voids and/or the lattice mismatch between Si and SiC of 20%. The presence of oriented structures with lateral dimensions of 40–80 nm is conformed, as shown Figure 4(b). The dark regions correspond to a stoichio-

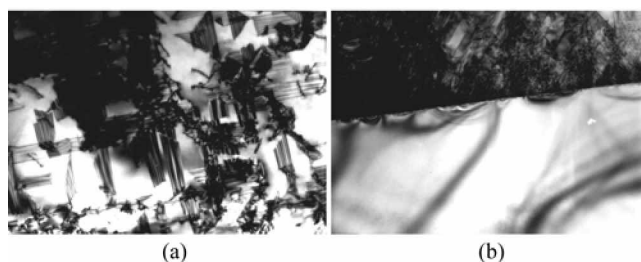


**Figure 4.** (a) Plane and (b) cross-sectional TEM images of 3C-SiC films grown on Si (100) substrates.

metric, but more disordered phase. The columnar structures appear to be nearly epitaxially close to the Si substrate. The grains twin in the normal direction, as suggested by their reduction in diameter when two neighboring columns join, even if the merging is prevented by the mismatch. As a matter of fact, a perfect mismatch at the interface can be realized in the presence of an edge dislocation, as theoretically postulated by Cicero *et al.*<sup>18</sup>

RHEED analysis was performed on 3C-SiC films grown to various thicknesses to characterize their crystallinity. Figure 5 shows RHEED patterns of 3C-SiC films grown on the Si (100) substrate along an  $\langle 100 \rangle$  azimuth for film thicknesses of Figure 5(a) 0.6, (b) 2.6, (c) 4.3 and (d) 12.8  $\mu\text{m}$ . With an increase in the 3C-SiC film thickness as shown in Figure 5, the RHEED patterns of the heteroepitaxially grown 3C-SiC films gradually changed from a spot pattern to a streak pattern without twin spots and indicated that single-crystalline cubic SiC (100) films were grown heteroepitaxially on the Si (100) wafer. These variations in RHEED patterns can be considered to be due to the decrease in the number of crystal defects such as twins, dislocations or other stacking faults. The XRD and RHEED results demonstrate that the crystallinity of 3C-SiC films improves as the films grew thicker.

Figures 6(a) and (b) show a photograph and an AFM image of the mirror like crystal surface of 3C-SiC films grown on Si (100) substrates. The grown 3C-SiC films had a mirror like surface with excellent flatness. The root mean square (RMS) roughness and roughness average (Ra) of the grown films were 8.2 and 6.6 nm, respectively; the films were very rough compared with that of mirror-like surface of the Si wafers. Moreover, ridges were observed on surfaces:

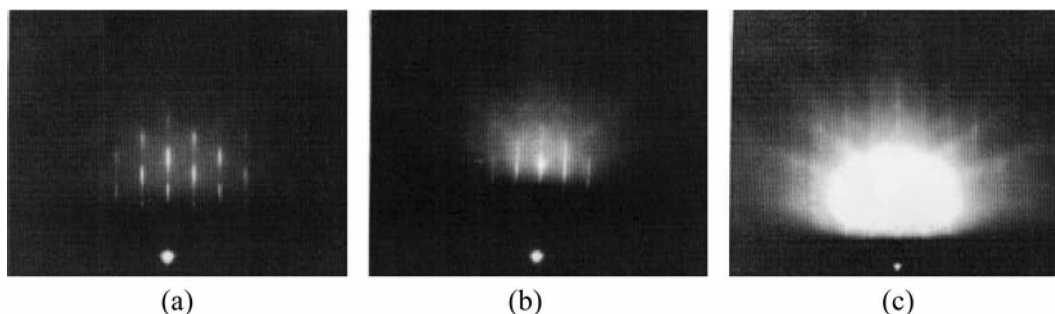


**Figure 5.** RHEED patterns of 3C-SiC films grown on on-axis Si (100) substrate along  $\langle 100 \rangle$  azimuth for film thicknesses of (a) 0.6, (b) 2.6, (c) 4.3 and (d) 12.8  $\mu\text{m}$ .

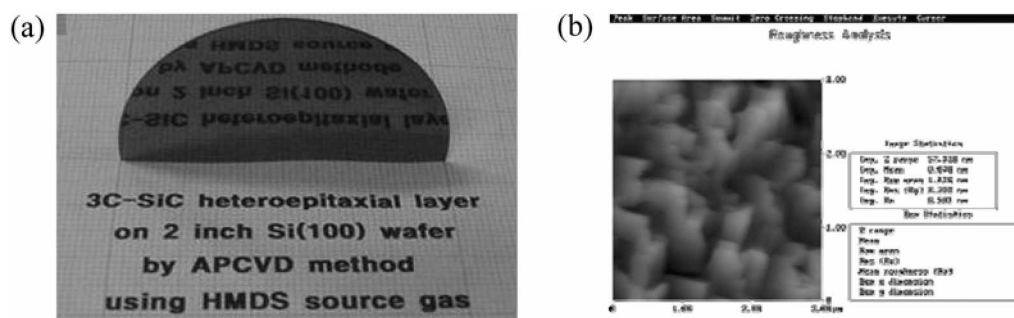


Figure 6. (a) Photograph and (b) AFM image of mirror surface of 0.6- $\mu\text{m}$ -thick 3C-SiC films grown on Si (100) substrate.

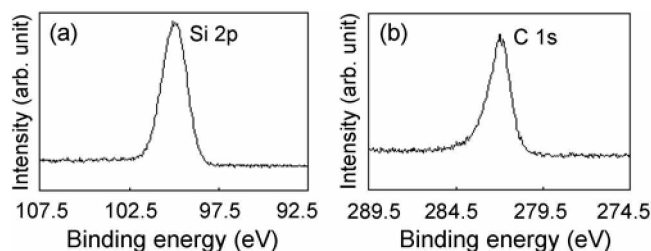


Figure 7. High-resolution XPS spectra of 3C-SiC thin films grown on Si (100) substrates: (a) Si 2p and (b) C 1s peaks.

these ridges were distributed [110] direction of the surface of the grown 3C-SiC films. The growth of ridges resulted in groove formation during carbonization. Surface roughness was also found to increase with film thickness.

Figure 7 shows typical XPS spectra of Si 2p and C 1s for the 3C-SiC films grown on Si (100) substrates. An XPS investigation was carried out using Al-K $\alpha$  (1486.6 eV) radiation of the x-ray accelerated voltage of 15 kV and power 150 W as excitation source of photon. All the measurements were performed at pressures lower than  $5 \times 10^{-8}$  Torr in the analysis chamber. The spot size for analysis was 500  $\mu\text{m}$ , and the wide- and narrow-scan step sizes were 1 and 0.05 eV, respectively. Corrections of the samples were made by taking C 1s and Si 2p in SiC's as references at 282.7 and 100.3 eV, respectively.<sup>19</sup> High-resolution XPS spectra for Si 2p and C 1s were obtained for all the 3C-SiC films at room temperature. The Si 2p spectra show a similar shape to the C 1s spectra and their peak bonding energies were 282.7 and 100.6 eV, respectively. These results were consistent with those of single-crystalline 3C-SiC films reported previously. This result indicates that the Si 2p peak at 100.6 eV and the C 1s peak at 282.7 eV correspond to the 3C-SiC phase. Therefore, the grown SiC films were synthesized as single crystals by SiC-C bonding.

Figure 8 shows typical Raman scattering spectra of the 9.1- $\mu\text{m}$ -thick 3C-SiC films grown on Si (100) substrates. Raman spectra were measured in backscattering geometry using a 5145- $\text{\AA}$ -line argon-ion laser at room temperature. The intensity of the transverse optical (TO) peak at 796  $\text{cm}^{-1}$  was less than that of the longitudinal optical (LO) peak at  $973 \pm 1$   $\text{cm}^{-1}$ . The appearance of the TO peak properly results from the rough surface of 3C-SiC films. However,

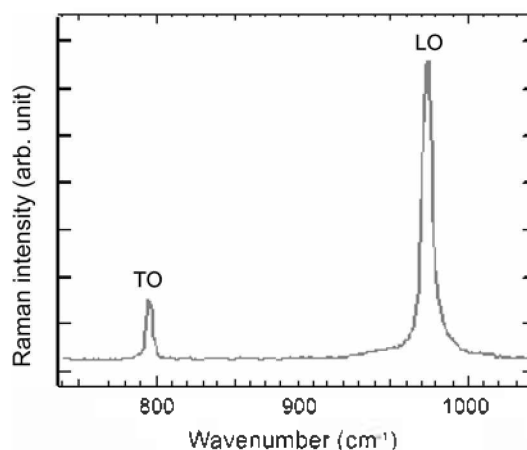


Figure 8. Typical Raman scattering spectra of 9.1- $\mu\text{m}$ -thick 3C-SiC films grown on Si (100) substrate.

the strong LO peak indicates that the grown 3C-SiC film results in a very good crystallinity. Moreover, with an increase in film thickness, the LO peak becomes sharper and stronger, which is characteristics of single crystals and 3C-SiC films with improved crystallinity. In addition, to evaluate the stress of heteroepitaxially grown 3C-SiC films, the 3C-SiC films were removed the Si substrate by etching with HF: HNO<sub>3</sub> = 1:1, and their Raman spectra was measured. The LO peak shifted from 973.2  $\text{cm}^{-1}$  to 974.52  $\text{cm}^{-1}$ . A tensile stress in the 3C-SiC film on the Si (100) substrate shifts the LO phonon to lower energy, and the 3C-SiC films became stress-free when the Si substrate was removed. The Raman shift between the 3C-SiC film s on the Si substrate and the free 3C-SiC films was 2  $\text{cm}^{-1}$ , corresponding to a biaxial stress range of 0.4-1 GPa and an inplane strain range of about 0.1-0.2%.<sup>21</sup> This result indicates that tensile biaxial stress is present in the grown 3C-SiC films due to the 20 % lattice mismatch between Si and SiC, as well as to the difference in thermal expansion coefficient between 3C-SiC and Si; the thermal coefficient of 3C-SiC is higher than that of Si.

## Conclusion

Single-crystalline 3C-SiC thin films have been heteroepitaxially grown on a Si (100) substrate using a single-

source precursor of HMDS as a safe organosilane source at 1350 °C by APCVD for M/NEMS applications. The crystalline quality of the grown 3C-SiC film was evaluated by XRD analysis, TEM, RHEED analysis, AFM, XPS, and Raman spectroscopy. It was confirmed that the main chemical components of the grown film were single-crystalline 3C-SiC. Moreover, the grown 3C-SiC film had a very good crystal without twins, defects or dislocations and a very low residual stress.

Therefore, 3C-SiC film grown on a Si (100) substrate have potential applications as mechanical and electrical materials for high power, high frequency, high optical, high radiation microelectronics and in biological fields. Moreover, they can be used in M/NEMS fields that operate in high temperatures and corrosive environments. RF, bio applications where current Si technologies cannot be employed.

**Acknowledgment.** This research was supported by the Program for the Training of Graduate Students in Regional Innovation which was conducted by the Ministry of Commerce Industry and Energy of the Korean Government.

### References

1. Kroetz, G. H.; Eickhoff, M. H.; Moeller, H. *Sens. Actuators A* **1999**, *74*, 182.
2. Casady, B.; Johnson, R. W. *Solid-State Electro.* **1996**, *39*, 1409.
3. Mehregany, M.; Zorman, C. A. *Thin Solid Films* **1999**, *355*, 518.
4. Sarro, P. M. *Sens. Actuators A* **2000**, *82*, 210.
5. Mehregany, M.; Zorman, C. A.; Roy, S.; Fleischman, A. J.; Wu, C. H.; Rajan, N. *Int. Mater. Rev.* **2000**, *45*, 85.
6. Yang, Y. T.; Ekinci, K. L.; Huang, X. M.; Schiavone, L. M.; Roukes, M. L. *Appl. Phys. Lett.* **2001**, *78*, 162.
7. Kotzar, G.; Freas, M.; Abel, P.; Fleischman, A.; Roy, S.; Zorman, C.; Moran, J. M.; Melzak, J. *Biomaterials* **2002**, *23*, 2737.
8. Badila, M.; Brezeanu, G.; Millan, J.; Godignon, P.; Locatelli, M. L.; Chante, J. P.; Lebedev, A.; Lungu, P.; Dinca, G.; Banu, V.; Banoiu, G.; Dia, G. *Related Materials* **2000**, *9*, 994.
9. Huang, X.; Zorman, C. A.; Mehregany, M.; Roukes, M. L. *Nature* **2003**, *421*, 496.
10. Eickhoff, M.; Moller, M.; Kroetz, G.; Stutzman, M. *J. Appl. Phys.* **2004**, *96*, 2872.
11. Nordell, N.; Nishino, S.; Yang, J. W.; Jacob, C.; Pirouz, P. *Appl. Phys. Lett.* **1994**, *64*, 1647.
12. Gao, D.; Wijesundara, B. J.; Carraro, C.; Howe, R. T.; Roya, M. *IEEE Sens. J.* **2004**, *4*, 441.
13. Jackson, K. M.; Dunning, J.; Zorman, C. A.; Mehregany, M.; Sharpe, W. N. *J. Microelectromechanical Sys.* **2005**, *14*, 664.
14. Ishida, Y.; Takahashi, T.; Okumura, H.; Yoshida, S.; Sekigawa, T. *Jpn. J. Appl. Phys.* **1997**, *36*, 6633.
15. Kim, K. C.; Shim, H. W.; Seo, Y. H.; Suth, E. K.; Nahm, K. S.; Lee, H. J. *J. Korean Phys. Soc.* **1998**, *32*, 588.
16. Wu, C. H.; Jacob, C.; Ning, X. J.; Nishino, S.; Pirouz, P. *J. Cryst. Growth* **1996**, *158*, 480.
17. Kubo, N.; Kawase, T.; Asahina, S.; Kanayama, N.; Tsuda, H.; Moritani, A.; Kitahara, K. *Jpn. J. Appl. Phys.* **2004**, *43*, 7654.
18. Cicero, G.; Pizzagalli, L.; Castellani, A. *Phys. Rev. Lett.* **2002**, *89*, 156.
19. Wijesundara, M. B. J.; Valente, G.; Ashurst, W. R.; Muthu, B. J.; Howe, R. T.; Pisano, A. P.; Carraro, C.; Roya, M. *J. of Electrochemical Soc.* **2004**, *151*, C210.
20. Kwon, J. H.; Youn, S. W.; Kang, Y. C. *Bull. Korean Chem. Soc.* **2006**, *27*, 1851.